Oxygenation of the Baltoscandian shelf linked to Ordovician biodiversification

Anders Lindskog [1,2] ✉, **Seth A. Young** [2], **Chelsie N. Bowman** [2], **Nevin P. Kozik** [2], **Sean M. Newby**[2], **Mats E. Eriksson**[1], **Johan Pettersson**[1], **Emmy Molin**[1] **& Jeremy D. Owens** [2]

Marine biodiversity increased markedly during the Ordovician Period (~487–443 million years ago). Some intervals within the Ordovician were associated with unusually rapid and prominent rises in taxonomic richness, the reasons for which remain debated. Links between increased oxygenation and biodiversification have been proposed, although supporting marine oxygen proxy data are limited. Here we present an expansive multi-site iodine-to-calcium (I/Ca) record from Lower–Middle Ordovician marine carbonates in Baltoscandia that provides a detailed account of the spatio-temporal development of oxygen conditions across this palaeoshelf. The data document progressive oxygenation of regional seafloor environments, with well-oxygenated waters sourced from the palaeoequatorward Iapetus Ocean and peak I/Ca values (that is, dissolved oxygen concentrations) coinciding with the most pronounced biodiversity increases and ecosystem reorganizations during this time interval. This occurred while the climate cooled, global sea level dropped and carbonate deposits became regionally dominant. The results suggest that ventilation of shelves played a critical role in regulating early Palaeozoic marine biodiversity via development of ecospace and aerobic–metabolic conditions.

The Ordovician Radiation, or Great Ordovician Biodiversification Event, resulted in global changes among marine ecosystems, as biodiversity increased and biota refined niche utilization. Marine life successively spread into and above the seafloor, throughout the water column, and trophic networks evolved[1]. Palaeontological datasets document a long-term rise in biodiversity with repeated bursts during which taxonomic richness rose rapidly[1–5]. The reasons for these pronounced increases in biodiversity have been debated, and explanatory scenarios commonly involve influences from climate change, oxygenation, tectonics and sea-level fluctuations[3,5,6]. Temperature proxy data indicate that the global climate cooled substantially during the Ordovician, and this change may have promoted evolution via more hospitable living conditions[7–10].

Ambient oxygen levels have had an important role in evolutionary history, as also implied by co-variation between modelled (atmospheric) oxygen levels and long-term biodiversity patterns throughout the Phanerozoic[11–13]. It has been postulated that rising oxygen concentrations had a fundamental effect on marine biodiversity during the Ordovician[14–16], but crude spatio-temporal resolution and scarce direct marine redox proxy investigations have hampered detailed interpretations. Oxygen levels in the atmosphere were likely relatively low during much of the early Palaeozoic, although there is discord between empirical data and geochemical models (and between models)[17,18]. The patchy and scant Ordovician geochemical data suggest generally lower oxygen availability in the shallow marine realm when compared to the Mesozoic–Cenozoic[18,19].

In recent years, advances have been made in the development of geochemical proxies that help to elucidate ancient environmental conditions at various spatio-temporal scales. With this, reconstruction of the redox evolution of marine environments through geologic time has

¹Department of Geology, Lund University, Lund, Sweden. ²Department of Earth, Ocean and Atmospheric Science–National High Magnetic Field Laboratory, Florida State University, Tallahassee, FL, USA. ✉e-mail: anders.lindskog@geol.lu.se
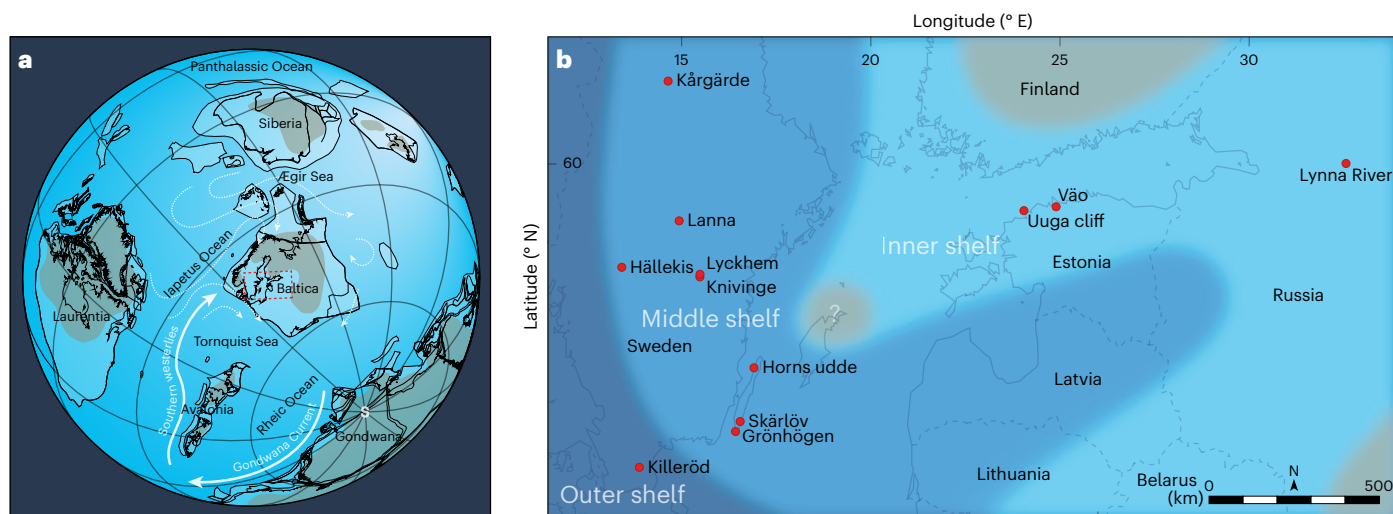
Fig. 1 | Palaeogeographic characteristics of the study area.
a, Palaeogeographic reconstruction for the Middle Ordovician (early Darriwilian, ~466 Ma), with names of notable continental masses and intercontinental seas and modelled upper ocean circulation[31] around Baltica indicated. Rectangle indicates area figured in **b**. The approximate distribution of land areas (tan-coloured shading) is generalized and simplified. **b**, Map of the Baltoscandian region, indicating the study localities (red dots) and notable features of the palaeoshelf as determined from relatively stable facies differentiation[8,25]. The areal distribution and extent of shelf features varied through time via influence from, for example, sea level and large-scale tectonics (main text and Supplementary Information section 2). Latitude and longitude refer to modern-day conditions. Panel **a** created with BugPlates (developed by T. H. Torsvik; www.geodynamics.no). Credits for basemap in **b**: data from Estonian Environment Agency (EEA), State Land Service of Latvia (VZD), Esri, Here, Garmin, Food and Agriculture Organization (FAO), National Oceanic and Atmospheric Administration (NOAA), United States Geological Survey (USGS); map created using ArcGIS software by Esri (www.esri.com).

become increasingly detailed. Iodine is redox-sensitive and among the earliest elements to be reduced under low-oxygen conditions in marine settings[19–21]. The dominant species of iodine in seawater are iodate (IO_3^-, oxidized) and iodide (I^-, reduced). Briefly and simplified, iodate can be structurally incorporated into carbonates whereas iodide cannot. Therefore, iodine concentrations can be used to assess marine oxygen conditions with the proxy expressed as iodine-to-calcium ratios (I/Ca) in carbonates. Such ratios are commonly reported as I/(Ca+Mg) to accommodate varying carbonate mineralogy; this is also done herein, but for brevity we use I/Ca notation. Studies in modern marine environments have established that I/Ca ratios >2.6 µmol mol^{-1} indicate locally well-oxygenated conditions[19–21]. Lower I/Ca ratios suggest at least some oxygen present, and <1.5 µmol mol^{-1} characterizes oxygen-limited conditions[22]. Here we apply a 1.5–2.6 µmol mol^{-1} transitional redox interval as a general reference. Although the long residence time of iodine entails similar concentrations in seas globally[20], in practice, I/Ca constitutes a local–regional proxy for the presence and proximity of oxygen-depleted waters. Hence, care should be taken before attempting to extrapolate data at a global scale[19]. The geographic limitation however has clear strengths in that I/Ca records conditions at the sampling site and the oxygen sensitivity of iodine makes it useful for establishing initial local redox responses. Other geochemical proxies, applicable to various lithologies, record global redox signals but are not necessarily reflective of local conditions[23]. Furthermore, such proxies typically respond to highly reducing conditions, limiting their capability to reconstruct subtle initial changes and variations close to the oxic–anoxic boundary across relatively small shelf areas, especially in carbonate settings[24].

Regional-scale systematic analyses of I/Ca in shelf carbonates have the potential to provide a detailed and nuanced spatio-temporal understanding of water-column redox conditions in relation to the timing and rates of Ordovician biodiversification. Such studies may also shed light on the connections among climate, oceanographic conditions and the habitability of shelf environments in deep time.

Iodine-to-calcium variations across the Baltoscandian palaeoshelf

The study sections represent an Early–Middle Ordovician regional shelf setting on the mid-latitude (~45° S) palaeocontinent of Baltica (Fig. 1). The sections form a biostratigraphically well-constrained transect across this shelf, going from shore proximal to distal roughly towards the present-day south and west (Figs. 1 and 2 and Supplementary Tables 1–12)[25,26]. Generally, low I/Ca values characterize the outer shelf. The most consistently high I/Ca values occur in the ~mid-shelf area. Eastward, I/Ca values are also relatively low. Long-term stratigraphic trends and shorter-term 'excursions' in I/Ca are consistent across the studied region—thus, the first-order stratigraphic patterns in I/Ca provide a faithful record of oxygen availability on the Baltoscandian shelf during the Early–Middle Ordovician. Differences between sections can largely be explained by varying proximity to a local–regional oxycline, oceanic connection/restriction, water depth and current regimes across the shelf, but diagenetic alteration may locally play a role in some stratigraphic horizons (Supplementary Information sections 1–3).

The basal Floian (Early Ordovician) I/Ca values span a relatively large range (~2–5 µmol mol^{-1}), indicating spatially variable oxygen conditions across the palaeoshelf. Higher values may be from very shallow-water environments related to the sedimentary break that commonly separates Floian strata from underlying rocks regionally (Fig. 2)[26–28]. The Floian thereafter is characterized by low I/Ca (~1–2), but values gradually increase towards a peak (~2.5–14.5) in the Floian–Dapingian (Early–Middle Ordovician) boundary interval. This suggests that water columns overlying Baltica transitioned from poorly to (near) well-oxygenated conditions through the Floian. Notably, the Floian–Dapingian transition, which appears to coincide with relatively low sea level, was associated with the expansion of carbonate sedimentation into many areas previously dominated by mudstone and shale[25–27].

A pronounced decline in I/Ca occurs in the lowermost Dapingian strata, suggesting a region-wide decrease in water-column oxygen contents (Fig. 2). I/Ca values then mainly increase throughout the Dapingian. Consistently high I/Ca values (maximum ~5–7.5) occur
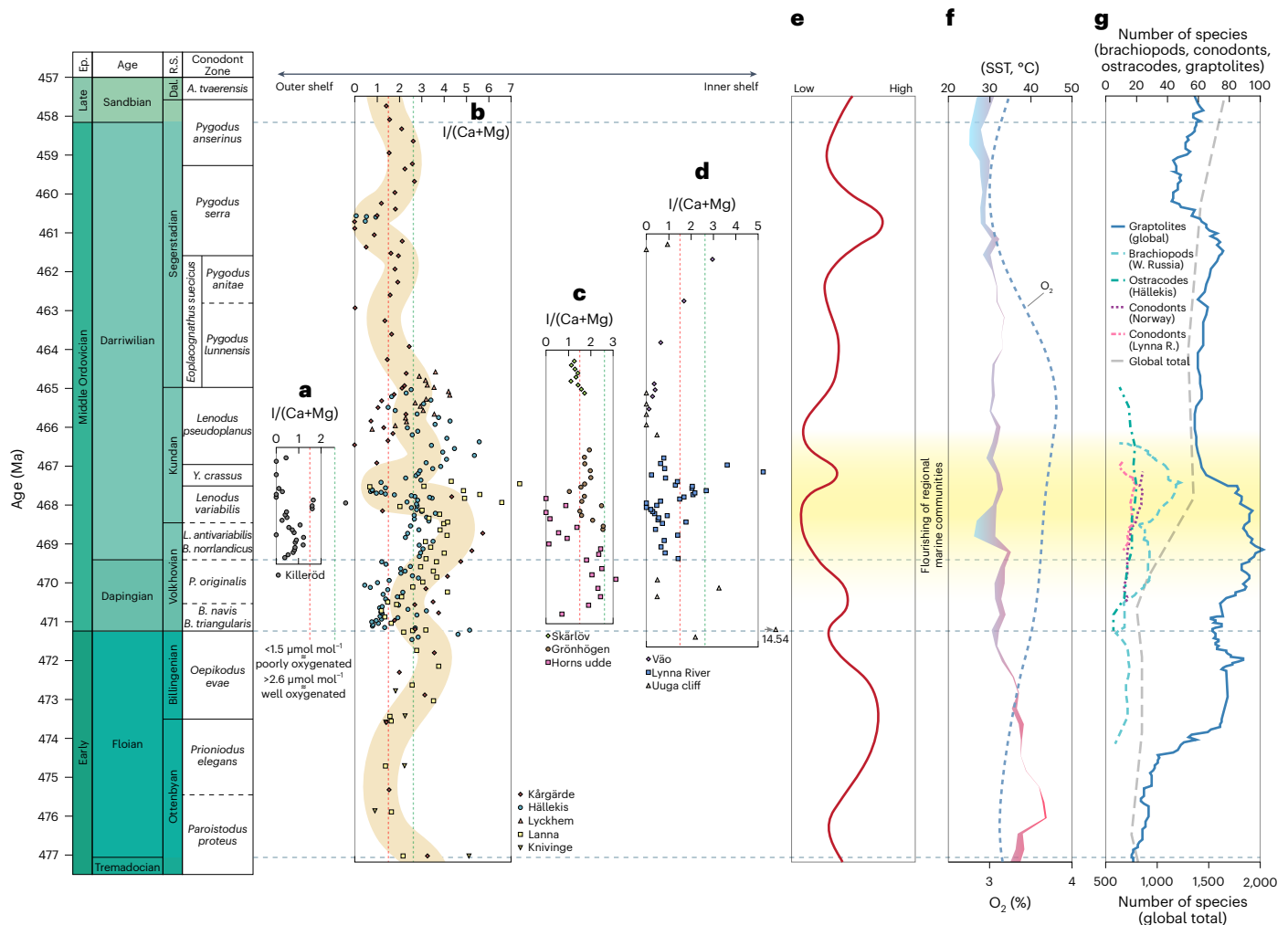
Fig. 2 | Compilation of iodine-to-calcium data, environmental parameters and biodiversity. All datasets scaled vertically according to biozonation (Supplementary Information section 3) and relative to the Geologic Time Scale 2020 (ref. 49), regional stages (R.S.) after Nielsen et al.[26]. Ma stands for million years ago; Ep. stands for epoch. Horizontal dashed lines indicate global Age (Stage) boundaries, for lateral reference; vertical dashed lines in **a**–**d** indicate transitional redox interval (I/Ca 1.5–2.6 μmol mol⁻¹; see main text). More positive I/Ca values indicate more dissolved oxygen in the marine environment. The data indicate that oxygen increased through the late Floian and into the early mid-Darriwilian, concurrently with major increases in marine biodiversity. All I/(Ca+Mg) data reported in μmol mol⁻¹; errors for individual measurements are smaller than the data symbols. **a**, I/(Ca+Mg), outer shelf (Fig. 1b). **b**, I/(Ca+Mg), middle shelf. A generalized interpretation of the main I/Ca trends indicated by shaded curve (tan-coloured field); the precision of this qualitative approximation

is limited by variations in data density. **c**, I/(Ca+Mg), middle–inner shelf. **d**, I/(Ca+Mg), inner shelf. One 'outlier' datapoint (14.5 μmol mol⁻¹) was omitted. **e**, Generalized sea-level curve (red line) showing presumed eustatic variations; composite after Nielsen[29], Rasmussen et al.[8], Lindskog and Eriksson[25], Rasmussen et al.[10] and Lindskog et al.[28,37], excluding high-resolution local variability. **f**, Global sea-surface temperature (SST) curve (coloured solid field) based on oxygen isotopes (δ¹⁸O), modified from lowest-temperature decile (that is, highest δ¹⁸O decile, presumed to be the diagenetically best preserved signal) reconstruction of Goldberg et al.[9] and atmospheric oxygen (O₂) modified from Krause et al.[17]. **g**, High-resolution biodiversity data from Tinn and Meidla (ostracodes)[36], Rasmussen et al. (brachiopods)[40], Cooper et al. (graptolites)[50], Rasmussen et al. (global total)[3], Lindskog et al. (conodonts, Lynna River)[37] and Rasmussen et al. (conodonts, Norway)[10].

regionally in upper Dapingian through middle Darriwilian strata, signalling a protracted time interval (~5 Myr) of well-oxygenated conditions across the shelf. This interval of sustained high I/Ca, which is most pronounced in the mid-shelf area, coincides with evidence of a marked drop in sea level[8,25,29]. A temporary episode of declining I/Ca (minimum ~0.7) occurs near the *Lenodus variabilis–Yangtzeplacognathus crassus* conodont zonal boundary (Fig. 2).

The upper half of the Darriwilian is characterized by a return to relatively low I/Ca values and purportedly oxygen-limited conditions (Fig. 2). The outer shelf saw a return to (black) shale deposition as sea level apparently rose[25–27,29].

Map projections of our I/Ca datasets indicate a gradual spreading of well-oxygenated waters that moved into the interior of Baltica throughout the Early–Middle Ordovician (Fig. 3a–h and Supplementary

Table 13). Oxygen-rich waters appear to have spread from the part of Baltica facing the Iapetus Ocean, roughly equatorward (Fig. 1)[30]. The regional I/Ca trends indicate that the mid-shelf area hosted the most consistently well-oxygenated environments, but the locus of apparent peak marine oxygen concentrations migrated through time. This may reflect prevailing shelf currents (Supplementary Table 14) and bathymetric conditions, which shifted with the paleogeographic configuration of Baltica and/or possibly with early stages of the Caledonian Orogeny[25,26,30] (Supplementary Information section 2).

Shelf oxygenation, biotic and environmental changes

The increase in oxygen availability indicated by I/Ca from the latest Floian through middle Darriwilian coincides with a successive series
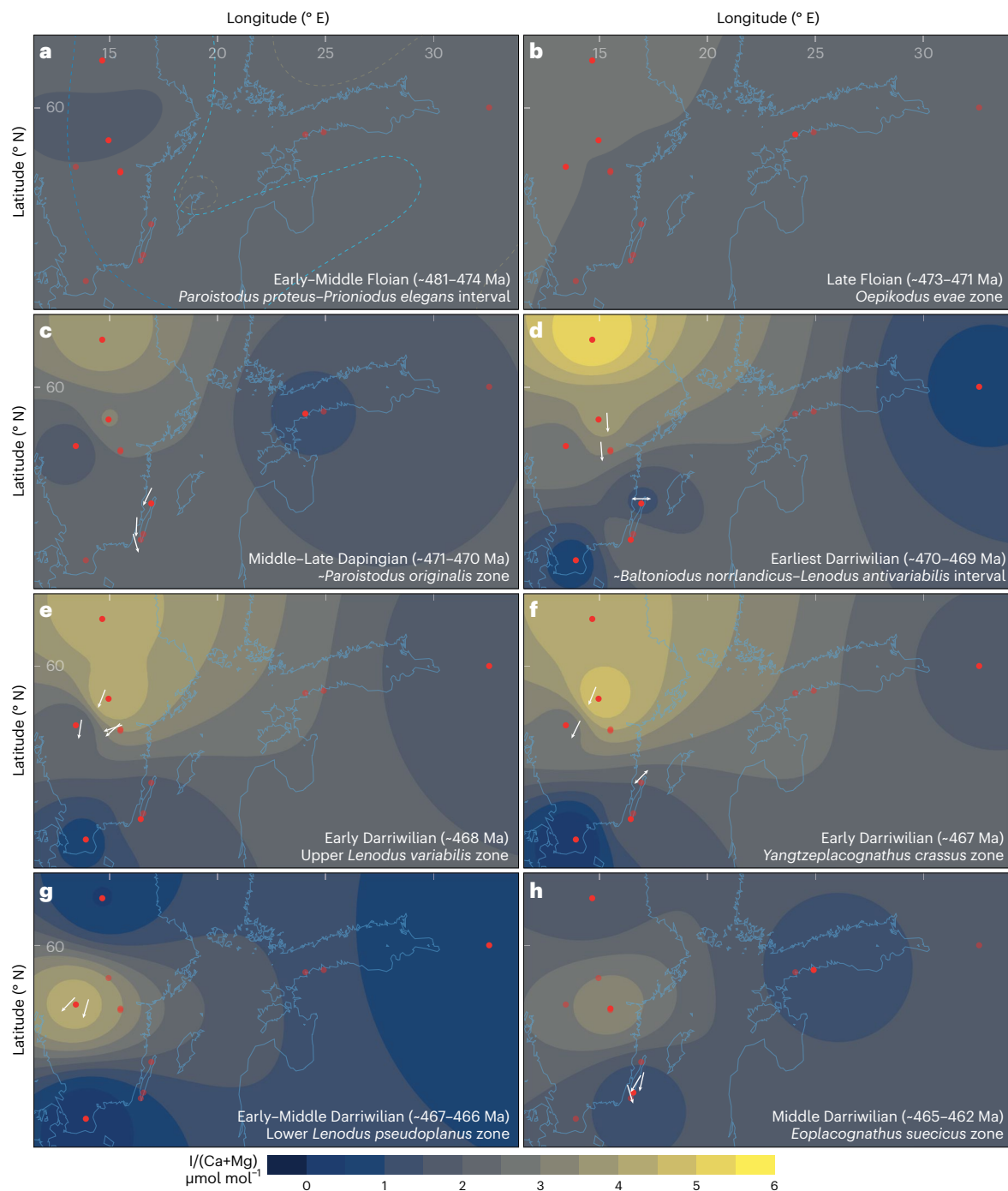
Fig. 3 | Spatio-temporal development of relative oxygen conditions in Baltoscandia. a–h, Time series illustrating the spatio-temporal development of relative oxygen conditions (I/Ca) across the Baltoscandian shelf. **a**, Stippled lines indicate generalized shelf features (Fig. 1b) for reference. Opaque red circles indicate localities included in data processing and map projections. Arrows indicate dominant water current directions, based on cephalopod conch orientations (Supplementary Information sections 2 and 5). The I/Ca data patterns indicate that the levels of dissolved oxygen increased in the shelf sea and that relatively oxygen-rich waters spread onto Baltica through time and migrated towards the south and west (modern-day directions). Credit: basemaps, data from EEA, VZD, Esri, Here, Garmin, FAO, NOAA, USGS; maps created using ArcGIS software by Esri (www.esri.com).

of biodiversity 'bursts' and behavioural innovations among benthic, nektic and planktic organisms (Fig. 2). Dominant regional patterns of marine taxonomic richness closely resemble the trends within our I/Ca datasets. Notably, global graptolite diversity is remarkably similar in stratigraphic patterns compared to I/Ca throughout the entire study interval, suggesting that well-oxygenated upper ocean water columns along continental margins played an important role in driving biodiversification among early Palaeozoic zooplankton. The coincidence

of major oceanic currents[31] (Fig. 1a) with the spatio-temporal patterns of I/Ca (Fig. 3) suggests that the source area of oxygen-rich waters was outside of Baltica. Thus, the Early–Middle Ordovician redox development on the Baltoscandian palaeoshelf was linked with events and processes at a broader, perhaps global, scale. Considering the relatively slow oxidation of iodide[19,22], the I/Ca data indicate that widespread oxidizing conditions were prevalent in water masses in the vicinity of Baltica. There are at present no directly comparable I/Ca datasets from

other parts of the world, but we note that our results agree with broadly correlative global redox proxy datasets[16,32] and models of atmospheric oxygen[14,17] that collectively suggest increasing oxygen during the late Floian–early Darriwilian and a decrease in the late Darriwilian (Fig. 2). This does however not imply that all parts of the global ocean experienced the same and synchronous development[33].

Peak I/Ca values at the Floian–Dapingian transition coincide with a regionally traceable hardground complex, colloquially termed 'Blommiga Bladet' (Sweden), 'Püstakkiht' (Estonia) and 'Steklo' (Russia)[26]. Innumerable bioerosional structures permeate the hardgrounds, with macroborings reaching unprecedented areal and volumetric density. The Floian–Dapingian boundary marks an important step in the global ichnofossil record as hardground-dwelling infaunal organisms became frequent at the macroscopic scale[34,35]. The pitted hardgrounds of Baltoscandia form a key example of this development. It is plausible that the combination of relatively slow sedimentation and elevated oxygen, which penetrated deeper into the seafloor, provided optimal conditions for behavioural experimentation (Fig. 3b,c). Potentially, an ambient marine oxygen threshold was passed, as younger strata are characterized by extensive bioturbation[25,28].

The long-duration interval of high I/Ca in the upper Dapingian–middle Darriwilian coincided with remarkable changes in the biotic and sedimentary records (Fig. 2). The corresponding time interval was characterized by a marked increase in taxonomic richness among marine organisms in the Baltoscandian region and high-resolution diversity patterns co-vary with trends in our I/Ca datasets (Fig. 2 and Supplementary Information section 2)[8,10,36,37]. As Ordovician biodiversification took off in earnest, the marine fauna of Baltoscandia flourished overall and regional seascapes became the scenes of richer and more varied ecosystems. Whereas preceding times were characterized by low-diversity, trilobite-dominated faunas (Fig. 3a), the Middle Ordovician saw a prominent influx of brachiopods, bryozoans, echinoderms and other sessile benthos and conodonts and molluscs[8,10,25,27–29,37–40] (notably, large cephalopods[41]; Fig. 3b–h). The flourishing of organisms is reflected in the composition of the strata via a marked increase in the proportion of skeletal grains as rock-forming components[25,27,28,37] (Supplementary Fig. 1), also apparent at the global scale[42]. Arguably, the expansion of oxygenated waters across the shelf (Fig. 3b–h) played a fundamental role in this biotic development (below).

The distinct drop in I/Ca near the *L. variabilis–Y. crassus* conodont zonal boundary coincides with the so-called Täljsten interval in Sweden, which is characterized by unusual litho- and biofacies (Fig. 2)[25]. Microbial fabrics and structures (oncoids, stromatolites) occur locally in Baltoscandia and possibly also globally[43,44]. Mass occurrences of *Sphaeronites* sp. cystoids (extinct echinoderms) are common, and this near-monospecific macrofauna has been interpreted as opportunistic colonization during adverse environmental conditions[25] (Supplementary Information section 2). The overall characteristics of the 'Täljsten' are consistent with dominantly reducing conditions at the seafloor and suggest temporary restriction of local depositional environments. The re-establishment of relatively low I/Ca values in the upper Darriwilian may reflect the global environmental development, with widespread formation of black shales[32].

Climate and oxygen catalysed Ordovician biodiversification

As sea level dropped globally through the late Floian–early Darriwilian, large areas of the Baltoscandian shelf probably became more influenced by hydrodynamic activity[25,28,39,44] that entailed more consistent and efficient mixing of atmospheric oxygen into marine environments. However, sea-level change alone does not suffice to explain the observed shift to well-oxygenated conditions in the study interval. This is because oxygen-rich waters appear to have encroached upon the shelf from the Iapetus Ocean (Fig. 3), but an off-shelf direction would be expected if oxygenation was a simple result of a shallowing water

column and migration of a regional oxygen minimum zone[15]. Hence, it is more likely that the progressive oxygenation reflects global-scale oceanographic changes[8,33]. It has been suggested that cooling sea surfaces and sea-level fluctuations during the Middle Ordovician were related, with the global climate state transitioning into 'icehouse'-like conditions[7,8,10]. Climatic cooling provides a plausible background to the oxygenation history of the Baltoscandian shelf, as changes in marine current regimes and strengthening of thermohaline circulation would be expected from global ocean temperature decline[8,31]. The palaeogeographic position of Baltica probably played an important role[33], as pervasive winds at mid-latitudes promoted mixing of atmospheric gasses into the regional shelf environment (Fig. 1a).

Cooling climate has repeatedly been promoted as a central driver behind Ordovician biodiversification[7,8,10], as have increasing oxygen levels[14]. These two interpretations are not mutually exclusive but rather complementary, as cooling would have allowed more dissolved oxygen in marine water columns. Indeed, the main trends in our I/Ca data are inverse to temperature estimates (Fig. 2 and Supplementary Information section 2). Climate and oxygen are intimately related through feedback processes at various spatio-temporal scales, and both strongly influence the distribution and organization of organisms[45–47]—thus, the combined effects of oceanic cooling and oxygenation provide a more holistic explanatory scenario for large-scale Ordovician biotic changes. A synergistic effect can be envisioned, wherein decreasing temperatures and rising oxygen levels expanded and stabilized the area and volume of habitable space via reduction of environmental and physiological hazards and stressors and enabled relatively energetic lifestyles[48]. Fundamentally, the net outcome was more balanced in terms of aerobic–metabolic requirements among the biota (Supplementary Information section 2).

Our study suggests that the Ordovician marine redox landscape was dynamic and evolving via multiple interacting mechanisms. It is likely that a combination of factors led to progressive radiation of marine life throughout the Ordovician, and spatio-temporal differences in biodiversity development at the global scale[1,4,5] paint a complex picture wherein dominant influences apparently varied between places and times. Nevertheless, at least on Baltica, several major biotic 'events' clearly coincide with I/Ca peaks and long-term trends, suggesting that oxygen indeed played an important role in evolutionary history during the Ordovician. Our I/Ca data are congruent with global models of oceanic oxygen conditions for the studied time interval[33], indicating clear linkages to Ordovician climate[9] and large-scale oceanic circulation[31]. Although seascapes differ, the inferred connections between climate and marine oxygenation in the Ordovician provide a glimpse into the future and the fate of modern shelf ecosystems as global temperatures rise.

Online content

Any methods, additional references, Nature Portfolio reporting summaries, source data, extended data, supplementary information, acknowledgements, peer review information; details of author contributions and competing interests; and statements of data and code availability are available at https://doi.org/10.1038/s41561-023-01287-z.

References

1. Webby, B. D., Paris, F., Droser, M. L. & Percival, I. G. *The Great Ordovician Biodiversification Event* (Columbia Univ. Press, 2004).
2. Sepkoski, J. J. J. in *Ordovician Odyssey: Short Papers for the Seventh International Symposium on the Ordovician System* (eds Cooper, J. D. et al.) 393–396 (Pacific Section Society for Sedimentary Geology, 1995).
3. Rasmussen, C. M. Ø., Kröger, B., Nielsen, M. L. & Colmenar, J. Cascading trend of Early Paleozoic marine radiations paused by Late Ordovician extinctions. *Proc. Natl Acad. Sci. USA* **116**, 7207–7213 (2019).

4. Deng, Y. et al. Timing and patterns of the Great Ordovician Biodiversification Event and Late Ordovician mass extinction: perspectives from South China. *Earth Sci. Rev.* **220**, 103743 (2021).

5. Servais, T., Cascales-Miñana, B. & Harper, D. A. T. The Great Ordovician Biodiversification Event (GOBE) is not a single event. *Paleontol. Res.* **25**, 315–328 (2021).

6. Stigall, A. L., Edwards, C. T., Freeman, R. L. & Rasmussen, C. M. Ø. Coordinated biotic and abiotic change during the Great Ordovician Biodiversification Event: Darriwilian assembly of Early Paleozoic building blocks. *Palaeogeogr. Palaeoclimatol. Palaeoecol.* **530**, 249–270 (2019).

7. Trotter, J. A., Williams, I. S., Barnes, C. R., Lécuyer, C. & Nicoll, R. S. Did cooling oceans trigger Ordovician biodiversification? Evidence from conodont thermometry. *Science* **321**, 550–554 (2008).

8. Rasmussen, C. M. Ø. et al. Onset of main Phanerozoic marine radiation sparked by emerging mid Ordovician icehouse. *Sci. Rep.* **6**, 18884 (2016).

9. Goldberg, S. L., Present, T. M., Finnegan, S. & Bergmann, K. D. A high-resolution record of early Paleozoic climate. *Proc. Natl Acad. Sci. USA* **118**, e2013083118 (2021).

10. Rasmussen, J. A., Thibault, N. & Rasmussen, C. M. Ø. Middle Ordovician astrochronology decouples asteroid breakup from glacially-induced biotic radiations. *Nat. Commun.* **12**, 6430 (2021).

11. Reinhard, C. T. et al. Earth's oxygen cycle and the evolution of animal life. *Proc. Natl Acad. Sci. USA* **113**, 8933–8938 (2016).

12. Large, R. R. et al. Atmosphere oxygen cycling through the Proterozoic and Phanerozoic. *Miner. Deposita* **54**, 485–506 (2019).

13. Riding, R., Liang, L., Lee, J.-H. & Virgone, A. Influence of dissolved oxygen on secular patterns of marine microbial carbonate abundance during the past 490 Myr. *Palaeogeogr. Palaeoclimatol. Palaeoecol.* **514**, 135–143 (2019).

14. Edwards, C. T., Saltzman, M. R., Royer, D. L. & Fike, D. A. Oxygenation as a driver of the Great Ordovician Biodiversification Event. *Nat. Geosci.* **10**, 925–929 (2017).

15. Edwards, C. T., Fike, D. A., Saltzman, M. R., Lu, W. & Lu, Z. Evidence for local and global redox conditions at an Early Ordovician (Tremadocian) mass extinction. *Earth Planet. Sci. Lett.* **481**, 125–135 (2018).

16. Kah, L. C., Thompson, C. K., Henderson, M. A. & Zhan, R. Behavior of marine sulfur in the Ordovician. *Palaeogeogr. Palaeoclimatol. Palaeoecol.* **458**, 133–153 (2016).

17. Krause, A. J. et al. Stepwise oxygenation of the Paleozoic atmosphere. *Nat. Commun.* **9**, 4081 (2018).

18. Brand, U. et al. Atmospheric oxygen of the Paleozoic. *Earth Sci. Rev.* **216**, 103560 (2021).

19. Lu, Z., Lu, W., Rickaby, R. E. M. & Thomas, E. *Elements in Geochemical Tracers in Earth System Science* (Cambridge Univ. Press, 2020).

20. Lu, Z., Jenkyns, H. C. & Rickaby, R. E. M. Iodine to calcium ratios in marine carbonate as a paleo-redox proxy during oceanic anoxic events. *Geology* **38**, 1107–1110 (2010).

21. Hardisty, D. S. et al. Perspectives on Proterozoic surface ocean redox from iodine contents in ancient and recent carbonate. *Earth Planet. Sci. Lett.* **463**, 159–170 (2017).

22. Hardisty, D. S. et al. Limited iodate reduction in shipboard seawater incubations from the Eastern Tropical North Pacific oxygen deficient zone. *Earth Planet. Sci. Lett.* **554**, 116676 (2021).

23. Owens, J. D. *Elements in Geochemical Tracers in Earth System Science 30* (Cambridge Univ. Press, 2020).

24. Tostevin, R. & Mills, B. J. W. Reconciling proxy records and models of Earth's oxygenation during the Neoproterozoic and Palaeozoic. *Interface Focus* **10**, 20190137 (2020).

25. Lindskog, A. & Eriksson, M. E. Megascopic processes reflected in the microscopic realm: sedimentary and biotic dynamics of the Middle Ordovician 'orthoceratite limestone' at Kinnekulle, Sweden. *GFF* **139**, 163–183 (2017).

26. Nielsen, A. T. et al. The Ordovician of Scandinavia: a revised regional stage classification. *Geol. Soc. London Spec. Publ.* **532**, 267–315 (2023).

27. Lindström, M. Vom anfang, hochstand und ende eines epikontinentalmeeres. *Geol. Rundsch.* **60**, 419–438 (1971).

28. Lindskog, A., Lindskog, A. M. L., Johansson, J. V., Ahlberg, P. & Eriksson, M. E. The Cambrian–Ordovician succession at Lanna, Närke, Sweden: stratigraphy and depositional environments. *Est. J. Earth Sci.* **67**, 133–148 (2018).

29. Nielsen, A. T. in *Ordovician of the world Publicaciones del Instituto Geológico y Minero de España, Cuadernos del Museo Geominero* (eds Gutiérrez-Marco, J. C. et al.) 399–401 (Instituto Geológico y Minero de España, 2011).

30. Torsvik, T. H. & Cocks, L. R. M. *Earth History and Palaeogeography* (Cambridge Univ. Press, 2016).

31. Pohl, A., Nardin, E., Vandenbroucke, T. R. A. & Donnadieu, Y. The Ordovician ocean circulation: a modern synthesis based on data and models. *Geol. Soc. London Spec. Publ.* **532**, SP532-2022-2021 (2023).

32. Zhang, J. et al. Progressive expansion of seafloor anoxia in the Middle to Late Ordovician Yangtze Sea: implications for concurrent decline of invertebrate diversity. *Earth Planet. Sci. Lett.* **598**, 117858 (2022).

33. Pohl, A. et al. Continental configuration controls ocean oxygenation during the Phanerozoic. *Nature* **608**, 523–527 (2022).

34. Ekdale, A. A., Benner, J. S., Bromley, R. G. & De Gibert, J. M. Bioerosion of lower Ordovician hardgrounds in southern Scandinavia and western North America. *Acta Geol. Hispanica* **37**, 9–13 (2002).

35. Mángano, M. G., Buatois, L. A., Wilson, M. & Droser, M. in *The Trace-Fossil Record of Major Evolutionary Events: Volume 1: Precambrian and Paleozoic* (eds Mángano, M. G. & Buatois, L. A.) 127–156 (Springer Netherlands, 2016).

36. Tinn, O. & Meidla, T. Middle Ordovician ostracods from the Lanna and Holen limestones, south-central Sweden. *GFF* **123**, 129–136 (2001).

37. Lindskog, A., Eriksson, M. E., Rasmussen, J. A., Dronov, A. & Rasmussen, C. M. Ø. Middle Ordovician carbonate facies development, conodont biostratigraphy and faunal diversity patterns at the Lynna River, northwestern Russia. *Est. J. Earth Sci.* **69**, 37–61 (2020).

38. Jaanusson, V. & Mutvei, H. *Ordovician of Öland. Guide to Excursion 3. IV International Symposium on the Ordovician System, Oslo 1982* (Swedish Museum of Natural History, 1982).

39. Lindström, M. Baltoscandic conodont life environments in the Ordovician: sedimentologic and paleogeographic evidence. *Geol. Soc. Am. Spec.* **196**, 33–42 (1984).

40. Rasmussen, C. M. Ø., Hansen, J. & Harper, D. A. T. Baltica: a mid Ordovician diversity hotspot. *Hist. Biol.* **19**, 255–261 (2007).

41. Kröger, B. Cambrian–Ordovician cephalopod palaeogeography and diversity. *Geol. Soc. London Mem.* **38**, 429–448 (2013).

42. Pruss, S. B., Finnegan, S., Fischer, W. W. & Knoll, A. H. Carbonates in skeleton-poor seas: new insights from Cambrian and Ordovician strata of Laurentia. *PALAIOS* **25**, 73–84 (2010).

43. Zhang, J. Lithofacies and stratigraphy of the Ordovician Guniutan Formation in its type area, China. *Geol. J.* **31**, 201–215 (1996).

44. Lindskog, A. Palaeoenvironmental significance of cool-water microbialites in the Darriwilian (Middle Ordovician) of Sweden. *Lethaia* **47**, 187–204 (2014).

45. Song, H., Wignall, P. B., Song, H., Dai, X. & Chu, D. Seawater temperature and dissolved oxygen over the past 500 million years. *J. Earth Sci.* **30**, 236–243 (2019).

46. Wade, D. C. et al. Simulating the climate response to atmospheric oxygen variability in the Phanerozoic: a focus on the Holocene, Cretaceous and Permian. *Clim. Past.* **15**, 1463–1483 (2019).

47. Stramma, L. & Schmidtko, S. Spatial and temporal variability of oceanic oxygen changes and underlying trends. *Atmos. Ocean* **59**, 122–132 (2021).

48. Vaquer-Sunyer, R. & Duarte, C. M. Temperature effects on oxygen thresholds for hypoxia in marine benthic organisms. *Glob. Change Biol.* **17**, 1788–1797 (2011).

49. Goldman, D. et al. in *Geologic Time Scale 2020* (eds Gradstein F. M. et al.) 631–694 (Elsevier, 2020).

50. Cooper, R. A., Sadler, P. M., Munnecke, A. & Crampton, J. S. Graptoloid evolutionary rates track Ordovician–Silurian global climate change. *Geol. Mag.* **151**, 349–364 (2014).

Methods

Samples were collected at the different localities during numerous field campaigns. Representative subsamples were selected for thin-section production (for visual screening) and preparation of sample powders (for geochemical analyses). The powders were produced via low-speed drilling of fresh, macroscopically well-preserved rock portions (multiple spots per sample for homogenization), using diamond-tipped microdrill bits that were cleaned with ethanol and dried with compressed air between individual samples. Reference sample materials are archived at the Department of Geology, Lund University.

I/(Ca+Mg) analyses were performed using standard procedures outlined by Lu et al.[19,20] and previous work from the Geochemistry Group at the National High Magnetic Field Laboratory at Florida State University[51–53]. Between 2 and 4 mg of carbonate powder was weighed into microcentrifuge tubes and dissolved in trace metal grade 3% HNO_3. Samples were then diluted with ultrapure 2% HNO_3 to create a matrix solution of 50 ± 5 ppm $[Ca^{2+}] + [Mg^{2+}]$. Analyses were performed on an Agilent 7500cs inductively coupled plasma mass spectrometer within 2 h of acidification (due to the volatility of iodine)[19–21]. The precision of ^{127}I is typically better than 2% and is not reported separately for individual samples. Standard deviation in counts per second (cps) for three blanks in a row is typically below 300 cps, and the sensitivity for a 1 part per billion standard is typically 60,000–120,000 cps depending on the instrument set-up each day (that is, sensitivity varies day to day, but the geostandards document consistent ratios). Calibration standards were continually made by serial dilution of a High-Purity Standards 10 ppm iodide inductively coupled plasma mass spectrometer standard and with a similar matrix of ~50 ppm Ca + Mg. The long-term accuracy of the analytical procedure was ensured via replicate measurements of known reference materials (KL1-2, KL1-4) and calculated to ± 0.5 µmol mol^{-1}.

Land outlines and national borders in Figs. 1b and 3 modified from 'Light Gray Canvas' basemap (www.arcgis.com/home/item.html?id=979c6cc89af9449cbeb5342a439c6a76). For the spatio-temporal reconstruction maps in Fig. 3, data series were subdivided according to biostratigraphy and average I/Ca values were calculated from the shortest possible intervals that can be resolved and used for relatively robust stratigraphic correlations (Supplementary Table 13). The reconstructions were produced using the Inverse Distance Weighted interpolation method (Geostatistical Analyst toolset; default settings with 'Power' set to 2.5) in Esri ArcGIS Pro 2.6. Localities without relevant strata (due to stratigraphic gaps, lack of sampling and so on) were omitted from individual analytical runs (Fig. 3). Due to lack of data, land extent and other possible topographic barriers on the palaeoshelf were not considered in the analyses. For further information on the Inverse Distance Weighted method, readers are referred to Esri's software documentation for ArcGIS.

Data availability

The datasets generated during this study are available in the associated Supplementary Information document. The analytical data are also accessible via the EarthChem online data repository at https://doi.org/10.26022/IEDA/113005.

References

51. Lowery, C. M. et al. Rapid recovery of life at ground zero of the end-Cretaceous mass extinction. *Nature* **558**, 288–291 (2018).
52. Bowman, C. N. et al. Integrated sedimentary, biotic, and paleoredox dynamics from multiple localities in southern Laurentia during the late Silurian (Ludfordian) extinction event. *Palaeogeogr. Palaeoclimatol. Palaeoecol.* **553**, 109799 (2020).
53. Kozik, N. P., Gill, B. C., Owens, J. D., Lyons, T. W. & Young, S. A. Geochemical records reveal protracted and differential marine redox change asssociated with Late Ordovician climate and mass extinctions. *AGU Adv.* **3**, e2021AV000563 (2022).

Author contributions

A.L. designed and planned the project with input from S.A.Y. and J.D.O. A.L., M.E.E., S.A.Y. and J.P. performed field sampling and measurements. A.L., J.P., E.M., C.N.B., N.P.K. and S.M.N. prepared laboratory samples. A.L., C.N.B., N.P.K. and S.M.N. performed I/Ca analyses. A.L. drafted the figures. The manuscript was mainly written by A.L., S.A.Y. and J.D.O, and the final draft was compiled with input from all co-authors.

Competing interests

The authors declare no competing interests.

Additional information

Supplementary information The online version contains supplementary material available at https://doi.org/10.1038/s41561-023-01287-z.

Correspondence and requests for materials should be addressed to Anders Lindskog.

Peer review information *Nature Geoscience* thanks Linda Kah, Junpeng Zhang and the other, anonymous, reviewer(s) for their contribution to the peer review of this work. Primary Handling Editors: Louise Hawkins and James Super, in collaboration with the *Nature Geoscience* team.

Reprints and permissions information is available at www.nature.com/reprints.